JOURNAL OF CATALYSIS **169,** 143–156 (1997)
ARTICLE NO. CA971653

In Situ Imaging of Catalytic Etching on Silver during Methanol Oxidation Conditions by Environmental Scanning Electron Microscopy

Graeme J. Millar,*[,1] Megan L. Nelson,* and Philippa J. R. Uwins†

*Department of Chemistry and †Centre for Microscopy and Microanalysis, The University of Queensland, St. Lucia, Brisbane, Queensland 4072, Australia

Received June 4, 1996; revised February 10, 1997; accepted February 11, 1997

Polycrystalline silver is used to catalytically oxidise methanol to formaldehyde. This paper reports the results of extensive investigations involving the use of environmental scanning electron microscopy (ESEM) to monitor structural changes in silver during simulated industrial reaction conditions. The interaction of oxygen, nitrogen, and water, either singly or in combination, with a silver catalyst at temperatures up to 973 K resulted in the appearance of a reconstructed silver surface. More spectacular was the effect an oxygen/methanol mixture had on the silver morphology. At a temperature of ca. 713 K pinholes were created in the vicinity of defects as a consequence of subsurface explosions. These holes gradually increased in size and large platelet features were created. Elevation of the catalyst temperature to 843 K facilitated the wholescale oxygen induced restructuring of the entire silver surface. Methanol reacted with subsurface oxygen to produce subsurface hydroxyl species which ultimately formed water in the subsurface layers of silver. The resultant hydrostatic pressure forced the silver surface to adopt a "hill and valley" conformation in order to minimise the surface free energy. Upon approaching typical industrial operating conditions widespread explosions occurred on the catalyst and it was also apparent that the silver surface was extremely mobile under the applied conditions. The interaction of methanol alone with silver resulted in the initial formation of pinholes primarily in the vicinity of defects, due to reaction with oxygen species incorporated in the catalyst during electrochemical synthesis. However, dramatic reduction in the hole concentration with time occurred as all the available oxygen became consumed. A remarkable correlation between formaldehyde production and hole concentration was found.

INTRODUCTION

The selective oxidation of methanol to formaldehyde represents a very important industrial catalytic process. Polycrystalline silver catalysts are still used extensively, despite the availability of the competing mixed iron oxide/molybdenum oxide system (1), due to their excellent selectivity and conversion efficiency (2). Traditionally, attention has been directed towards the elucidation of the mechanism for ethylene epoxidation on silver catalysts (3, 4). Nevertheless, in recent years a resurgence of interest in the methanol oxidation process has occurred which has resulted in several groups focusing their research on this area (5–8). Wachs and Madix (9) presented a detailed mechanism based on experiments performed at relatively low temperatures on an Ag(110) single crystal. However, complications arise when polycrystalline silver catalysts operating under typical high temperature (923–973 K) conditions in an oxygen/methanol atmosphere are studied. It is well known that the nature of the reduction and oxidation procedure employed can cause substantial changes in the structure and adsorption properties of silver (10–12). Plischke and Vannice (11) noted that the reduction temperature used could significantly influence subsequent oxygen adsorption, a view also shared by Meima *et al.* (13). Lefferts *et al.* (14) concluded that hydroxyl species were formed in the subsurface region of polycrystalline silver as a consequence of interaction between hydrogen and subsurface oxygen. In addition, they proposed that defects in the silver surface were beneficial for subsurface oxygen and hydroxyl formation. Pinhole creation due to the interaction of methanol and oxygen has been reported by several authors (14–16) and is postulated to occur as a result of reaction between dissolved hydroxyl species (15, 16).

Clearly, complex morphological changes happen during the partial oxidation of methanol to formaldehyde on silver catalyst. Ideally, the actual reaction should be investigated under typical industrial conditions. Recently, we have developed the technique of environmental scanning electron microscopy (ESEM) to allow imaging of a catalyst under high temperature and pressure conditions (16). ESEM is unusual in that it actually uses the gaseous atmosphere as a mechanism both to collect the secondary electron signal and to neutralize any charge buildup on an insulating surface (17). Consequently, this paper reports an *in situ* ESEM investigation of methanol oxidation on polycrystalline silver catalyst. Raman microscopy was also employed to characterize the adsorbed species on the catalyst, before and after reaction.

[1] E-mail: millar@chem.chemistry.uq.oz.au.

0021-9517/97 $25.00

EXPERIMENTAL

Polycrystalline silver catalyst which had been synthesized by electrochemical methods was supplied by ICI Resins, New Zealand. An ICP analysis indicated that it was at least 99.99% pure and the BET surface area was ca. 50 $cm^2\ g^{-1}$. ESEM images were collected using an Electroscan ESEM model 20A instrument and an accelerating voltage of 30 kV. The analytical chamber was equipped with a heating stage attachment which could be accurately controlled between the values of 298 and 1273 K and typically samples were heated at a rate of ca. 5–10 K/min. An auxiliary valve allowed a flow of 100% O_2, CH_3OH (BDH, AnalaR Grade), O_2/H_2O, or O_2/CH_3OH (produced using a bubbler system operating at ca. 313 K) to be contacted with the catalyst. Images were continuously recorded with a conventional video camera and individual "snapshots" taken with a videoprinter. Typically, a loading of ca. 400 mg of silver was placed on the heating stage and the chamber pressure was manipulated to a value of between 320 and 800 Pa. The finer details of the silver catalyst were examined pre- and postreaction by a JEOL 890 field emission scanning electron microscope (FESEM).

The pinhole concentration in silver catalysts was determined by conventional image analysis software and defined as the number of holes per unit area of silver.

Raman spectra were acquired with a Renishaw Raman microprobe spectrometer equipped with a He–Ne laser operating at a power of ca. 1 mW at the sample, and a CCD detector. Spectra were averaged over 4 scans and recorded at a resolution of 4 cm^{-1}. Data manipulation was achieved using Grams Research software (Galactic Industries). All spectral measurements were performed at ambient temperature.

RESULTS

Characterization of "Fresh" Catalyst

A series of locations on the silver catalyst were probed by Raman microscopy and a selection of the spectra recorded are displayed in Fig. 1. In each spectrum the dominant feature was a strong band at ca. 230 cm^{-1} which was distinctly asymmetric in shape, suggesting the presence of another peak in the lower wavenumber region. Kondarides *et al.* (18) reported a band at 240 cm^{-1} following oxygen adsorption at 573 K on silver which was assigned to either a ν(Ag–O) or ν(Ag–O_2) vibration. Benndorf *et al.* (19) observed a feature at 220 cm^{-1} in the EELS spectrum of oxygen adsorbed on Ag(111), indicative of the ν(Ag–O) mode of dissociatively adsorbed oxygen. Moreover, Sexton and Madix (20) noted the appearance of a band at 240 cm^{-1} after O_2 exposure to Ag(110), which was assigned to the ν(Ag–O_2) vibration for molecularly bound oxygen. Consequently, the maximum at ca. 230 cm^{-1} in this study is proposed to be a combination of vibrations for both atomically and molecularly adsorbed oxygen on silver. Similarly, the shoulder at ca. 335 cm^{-1} compares to a peak at 325 cm^{-1} ascribed to atomic oxygen bound to Ag(110) (20).

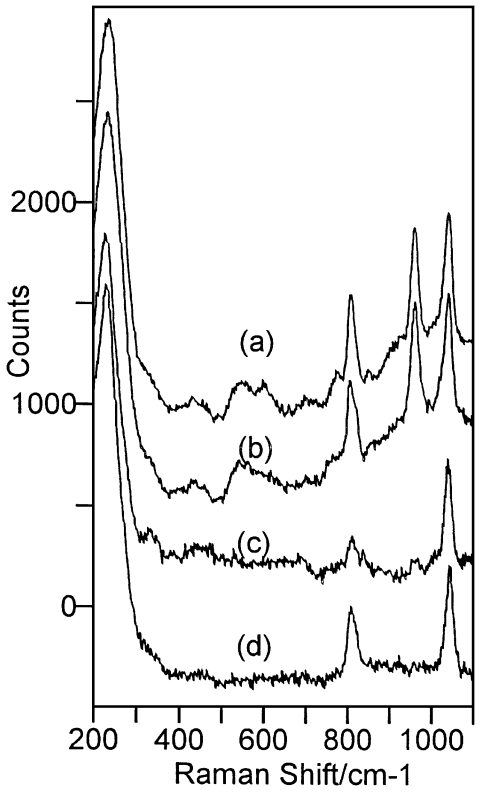

FIG. 1. Raman spectra of various locations on the surface of electrochemically synthesised polycrystalline silver catalyst.

A sharp peak at 1054 cm^{-1} was present in every spectrum which was characteristic for the ν_1 vibration of adsorbed carbonate (produced by reaction of CO_2 with chemisorbed atomic oxygen (21)). Figures 1a and 1b show the presence of a band at 965 cm^{-1}. Millar *et al.* (22) previously noted the presence of a peak at 960 cm^{-1} attributed to the ν(O–O) mode of molecular oxygen strongly bound to reconstructed silver sites, which is in accord with the band observed here.

Ertl and co-workers (23, 24) demonstrated that an oxygen-reconstructed silver single crystal displayed Raman bands at ca. 630 and 803 cm^{-1} assigned to the ν(Ag–O) vibrations for subsurface and strongly bound atomic oxygen species, respectively. Corresponding peaks have also been observed in Raman spectra of polycrystalline silver catalysts (22) and significantly their vibrational frequency was influenced by the presence of other adsorbates. Figures 1a and 1b exhibit broad maxima in the range 490–650 cm^{-1} which can be deconvoluted into 3 subbands at ca. 520, 570, and 605 cm^{-1}. Bao *et al.* (25) exposed either water or hydrogen to an oxidized Ag(111) single crystal to produce species identified by Raman bands at 554 cm^{-1} and 575 cm^{-1}. These

peaks were ascribed to the ν(Ag–O) modes of surface and subsurface hydroxyl species, respectively. Recently, Millar *et al.* (26) determined that subsurface hydroxyl species in polycrystalline silver were represented by a band at ca. 570 cm^{-1} whereas surface hydroxyl moieties were characterized by a peak at ca. 520 cm^{-1}. In relation to the observation of hydroxyl species it is interesting to note that a peak at ca. 780 cm^{-1} concomitantly appeared (Figs. 1a and 1b). Bao *et al.* (25) attributed a band at 985 cm^{-1} present after water interaction with silver to the δ(OH) mode of a hydroxyl species. Therefore, the current band at 780 cm^{-1} is unlikely to be due to a vibration for hydroxyl species. This deduction is in accordance with spectra which have contained an intense band at ca. 570 cm^{-1} typical of subsurface hydroxyl but no corresponding feature at ca. 780 cm^{-1} (26). However, it has been shown that formation of subsurface hydroxyl species from subsurface oxygen induces changes in the bonding between strongly adsorbed atomic oxygen and the reconstructed silver surface. In particular, a shift in the 810 cm^{-1} band to a lower wavenumber was observed (22). Similarly, the 605 cm^{-1} band is ascribed to subsurface oxygen species whose bonding has been influence by the presence of neighboring subsurface hydroxyl species.

There remains one last feature to assign: each spectrum contains a weak band at ca. 445 cm^{-1} (Fig. 1). A previous *in situ* Raman experiment has shown that the intensity of this band can increase substantially during methanol oxidation (22). Theoretical calculations by Carter and Goddard (27) predict that the ν(Ag–O) frequency for hydroxyl species adsorbed on silver should be 445 cm^{-1}, which strongly supports assignment of the 445 cm^{-1} feature to hydroxyl species. Consequently, one must differentiate between this species and those represented by peaks at ca. 520 and 570 cm^{-1}. Lefferts *et al.* (14) discovered from TPR measurements that hydroxyl species located in the vicinity of surface defects behaved differently from those created below a more ordered silver surface. Thus we propose that the band at 445 cm^{-1} is characteristic for the ν(Ag–O) mode of subsurface hydroxyl species present at defect sites. This assignment is supported by the fact that Bao *et al.* (25) did not observe this peak on a silver single crystal. A summary of the Raman assignments is provided in Table 1.

Electron microscopy revealed that the silver sample studied consisted of relatively large grains on the order of a few millimeters in diameter. The silver topology was relatively smooth although a significant number of defects in the microstructure could also be observed. Images of the fresh catalyst can be seen in Figs. 2a, 2c, and 3a.

Interaction of N_2 with Silver Catalyst

Figures 2a and 2b show images obtained from polycrystalline silver before and after exposure to an atmosphere of nitrogen at 973 K. In general, the original defect structures in the sample became less pronounced after thermal treatment in nitrogen. In addition, a very small concentration of "pinholes" appeared in the silver surface. Due to evaporation of the silver at the high exposure temperature (15), a distinct "hill and valley" structure was created over the catalyst surface (this effect is most easily seen by inspection of the particle in the lower right-hand corner of the image in Fig. 2b).

TABLE 1

Raman Band Positions for Oxygen Species Detected in Electrochemically Produced Polycrystalline Silver Catalyst

Band position	Species
230 cm^{-1}	Weakly adsorbed molecular oxygen and/or atomic oxygen on Ag(111)
335 cm^{-1}	Atomic oxygen adsorbed on Ag(110)
445 cm^{-1}	Subsurface hydroxyl (defect sites)
520 cm^{-1}	Surface hydroxyl
570 cm^{-1}	Subsurface hydroxyl (extended surface planes)
605 cm^{-1}	Subsurface oxygen (shifted by neighbouring subsurface hydroxyl groups)
780 cm^{-1}	Strongly bound atomic oxygen (shifted because of co-adsorbates)
965 cm^{-1}	Strongly adsorbed molecular oxygen (at reconstructed surface)
1054 cm^{-1}	Adsorbed carbonate

Interaction of O_2 with Silver Catalyst

To investigate the effect of oxygen upon the structure of silver catalyst, a sample was treated in oxygen at 973 K (Figs. 2c and 2d). Clearly, the presence of oxygen influenced the morphology of silver since widespread surface reconstruction was observed (cf. Figs. 2b and 2d). This effect has been reported in detail by Ertl and co-workers (15, 28) who have shown that oxygen incorporation into subsurface locations leads to extensive restructuring of a silver surface.

Interaction of H_2O with Silver Catalyst

An experiment was performed to determine the effect of exposure to water vapour (a component of a methanol oxidation feedstock) upon the silver catalyst morphology. The silver catalyst was heated in H_2O vapour to a temperature of 973 K in the ESEM chamber and images were continuously acquired. All the pertinent structural changes are adequately illustrated by the "before" and "after" images shown in Figs. 3a and 3b. A general observation is that the particles possess a smoother texture following reaction. In addition, restructuring of the surface appears to have occurred as evidenced by the distinct surface facetting observed.

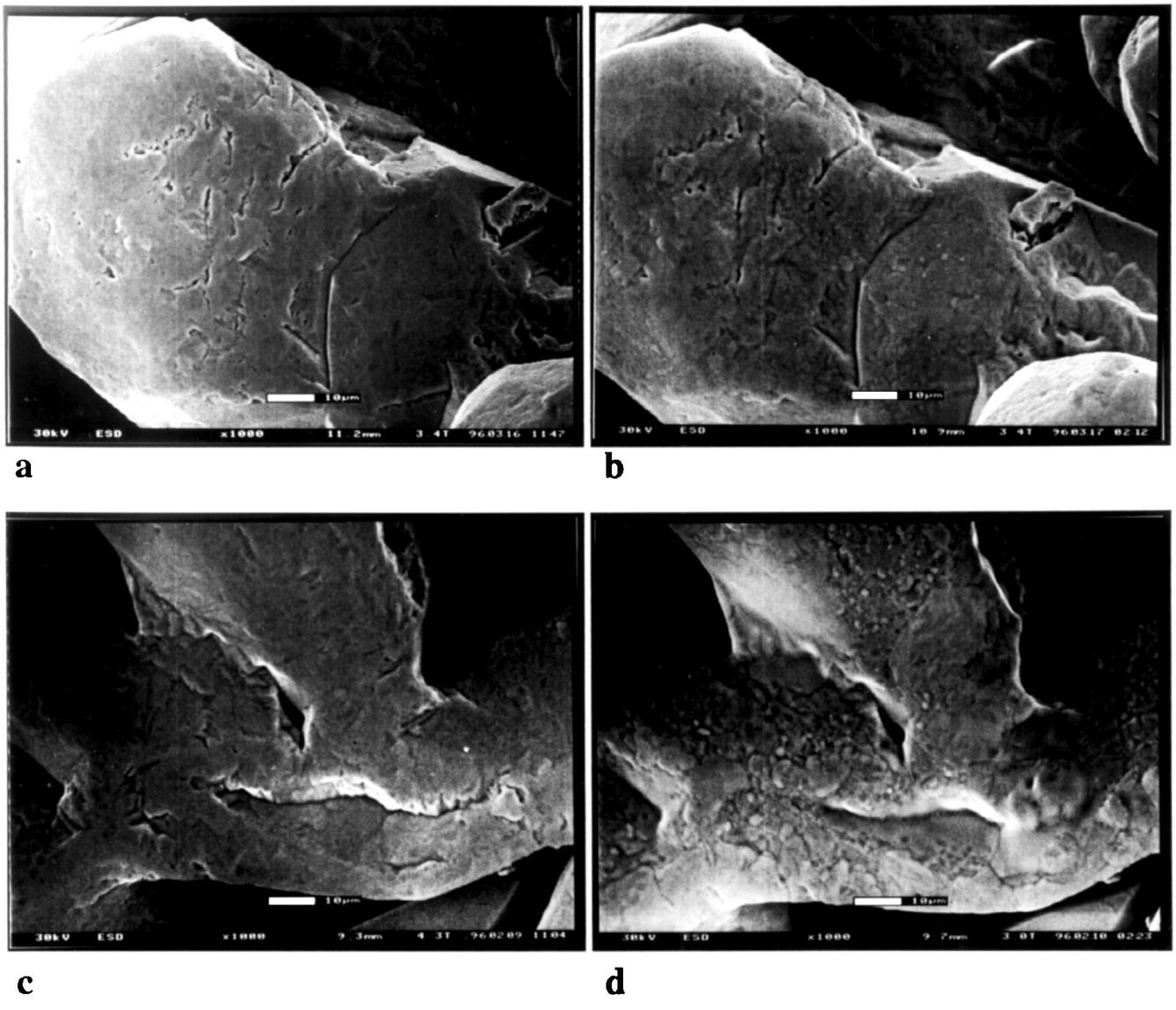

FIG. 2. Photos (a) and (b) are ESEM images of the silver catalyst before and after exposure to an atmosphere of nitrogen at 973 K. Photos (c) and (d) are ESEM images of the silver catalyst before and after exposure to an atmosphere of oxygen at 973 K.

Interaction of O_2/H_2O with Silver Catalyst

Ertl and co-workers (25) have demonstrated that the presence of water can substantially increase the rate of oxygen reconstruction of a silver surface. Consequently, an experiment was conducted where oxygen was passed through a water saturator before entering the ESEM chamber. As before, the silver sample was heated in the presence of this gaseous mixture to a temperature of 973 K (Figs. 3c, 3d). From the images obtained it was apparent that wholescale surface reconstruction was again induced, although it was difficult to unequivocally determine whether the presence of water did indeed alter the rate of reconstruction in the present situation.

Interaction of CH_3OH with Silver Catalyst

An ESEM experiment was conducted wherein methanol vapor was continuously exposed to a silver catalyst which was heated to a temperature of 973 K (Fig. 4). No discernible changes in the catalyst morphology were evident until the sample temperature reached ca. 673 K (Fig. 4c) where a small concentration of "pinholes" was created. Further heating to 708 K resulted in a slight increase in the number of "pinholes" detected (Fig. 4d). Raising the catalyst temperature to 763 K (Fig. 4f) significantly accelerated the rate of "pinhole" formation. Furthermore, it was apparent that the holes were not randomly distributed but rather they appeared to be associated with defects in the silver surface. This latter observation is in accord with the study

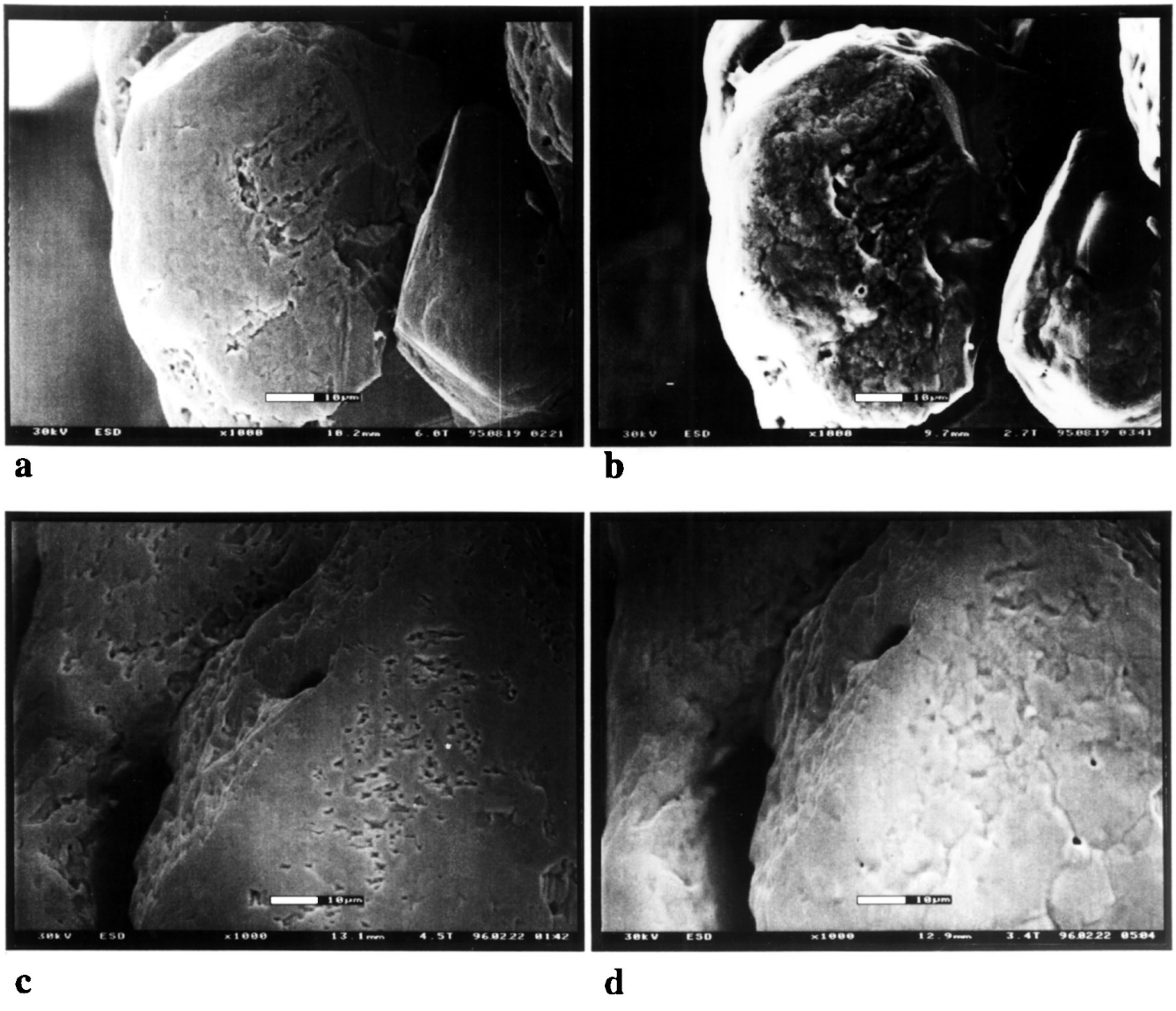

FIG. 3. Photos (a) and (b) are ESEM images of the silver catalyst before and after exposure to an atmosphere of water vapor at 973 K. Photos (c) and (d) are ESEM images of the silver catalyst before and after exposure to an atmosphere of oxygen and water vapor at 973 K.

by Lefferts *et al.* (14) which emphasized the possible importance of defects in polycrystalline silver upon the nature of adsorbate bonding. At 803 K (Fig. 4g) the extent of hole production maximized and it was also discerned that the original silver surface had reconstructed to produce large platelet structures. Importantly, "pinholes" were identified at the edges of these platelets which again suggests a relationship between the appearance of these two features.

As the catalyst temperature was further elevated to 973 K (Figs. 4h–4k) several changes in the surface morphology were identified. First, the "pinhole" concentration substantially diminished. Indeed, following extended methanol interaction at 973 K (Fig. 4l), the number of "pinholes" remaining was relatively insignificant. Second, much of the pronounced platelet structure formed at lower temperatures disappeared which suggests that the silver surface was very mobile under the applied high temperature conditions. Third, surface restructuring of the type seen when silver catalyst was contacted with oxygen or water vapor (cf. Figs. 3 and 4) was imaged.

Interaction of CH_3OH/O_2 with Silver Catalyst

Silver catalyst was placed in the ESEM chamber and subsequently heated in a flow of CH_3OH/O_2 to 973 K, at which time the catalyst was kept at that temperature for a further 41 min. A series of images displaying the critical changes in catalyst morphology during the reaction are presented in Fig. 5. The first notable change in catalyst structure occurred at ca. 713 K (Fig. 5b) where "pinhole" formation was observed. Significantly, these holes were all concentrated

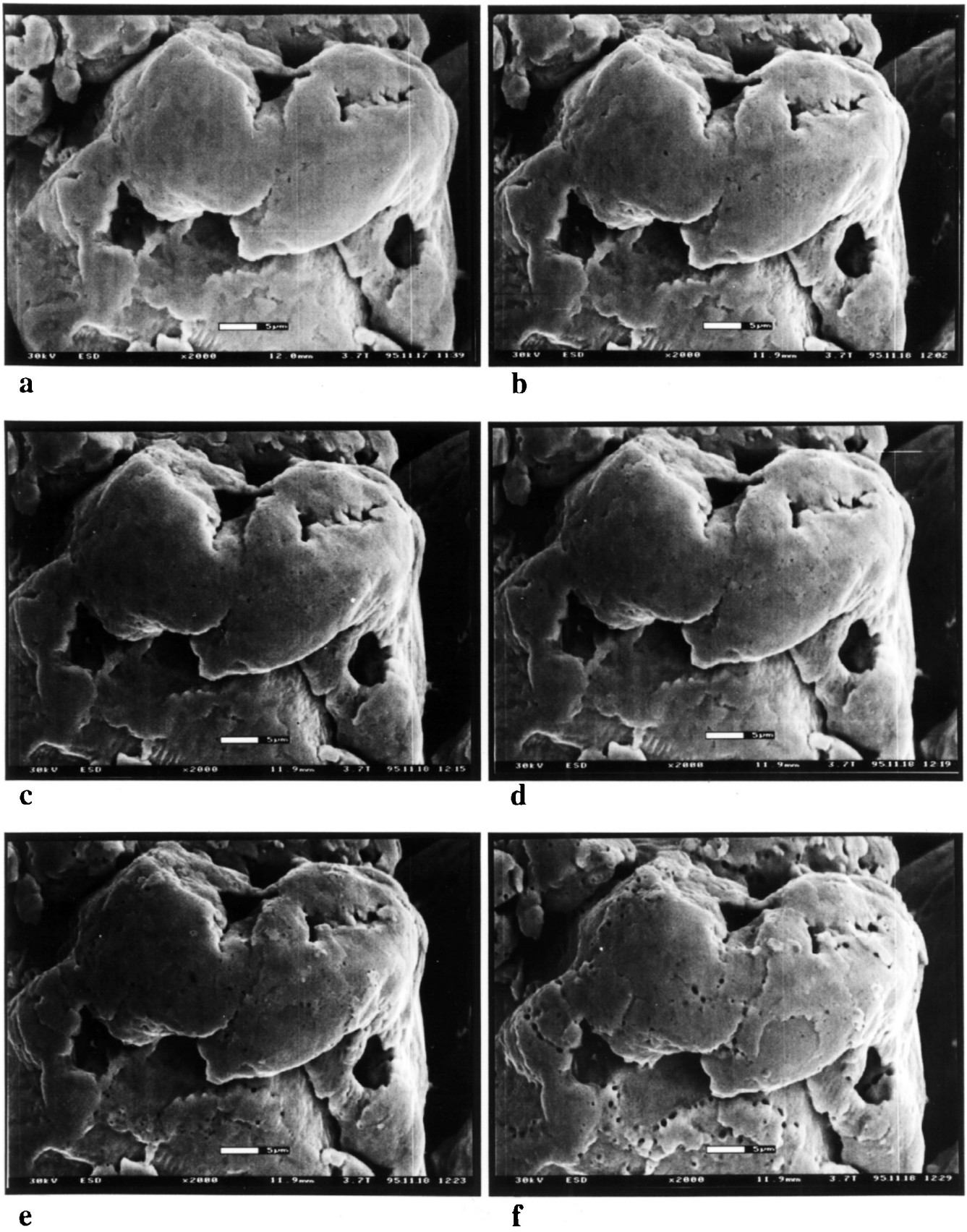

FIG. 4. Real time ESEM images of polycrystalline silver catalyst in methanol vapor at (a) 298, (b) 568, (c) 673, (d) 708, (e) 735, (f) 763, (g) 803, (h) 853, (i) 878, (j) 942, and (k) 973 K. Photo (l) shows the catalyst structure after holding the catalyst at a temperature of 973 K in methanol vapor for a further 1 h.

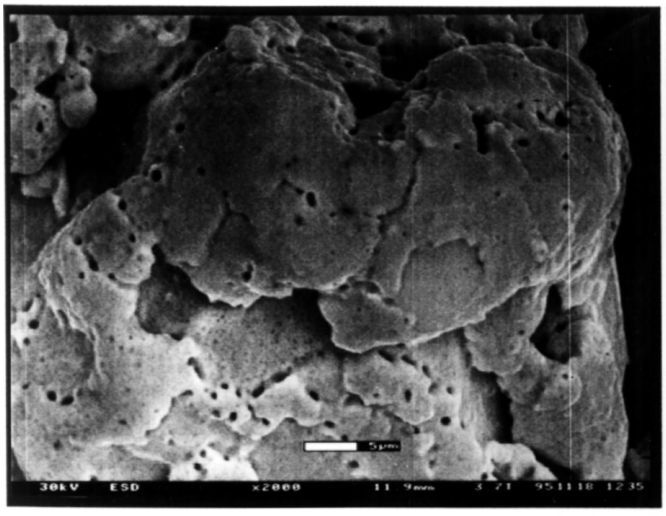

g

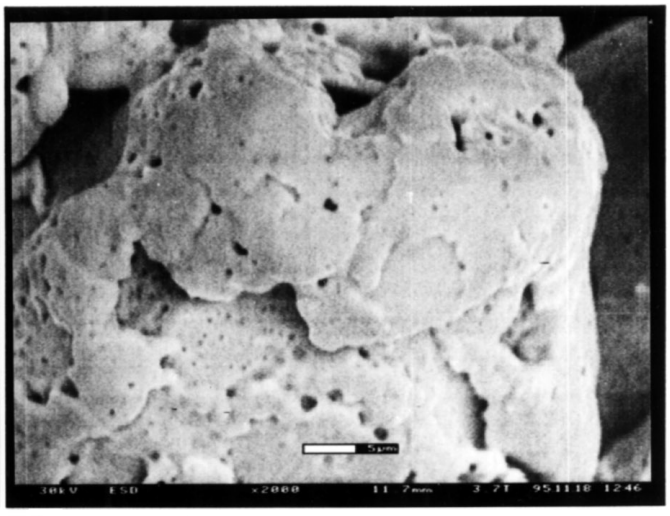

h

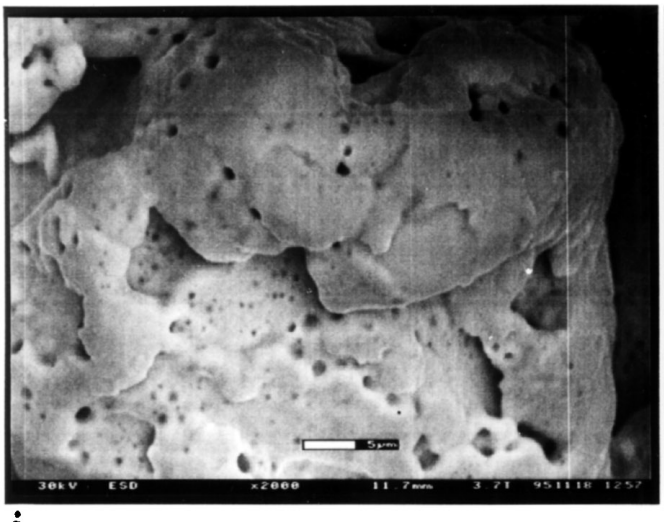

i

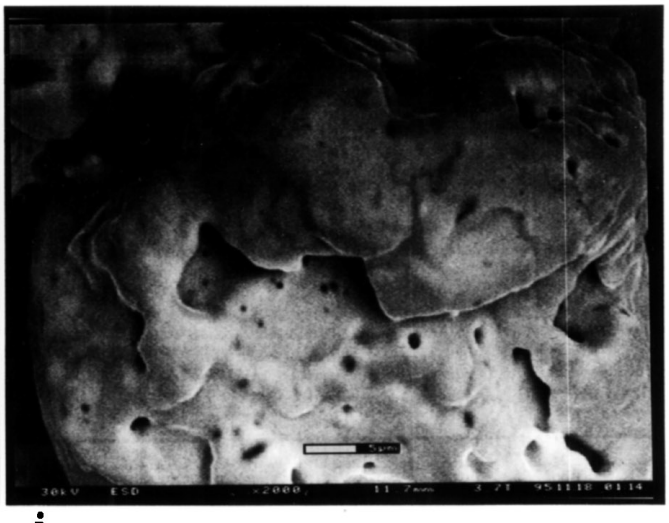

j

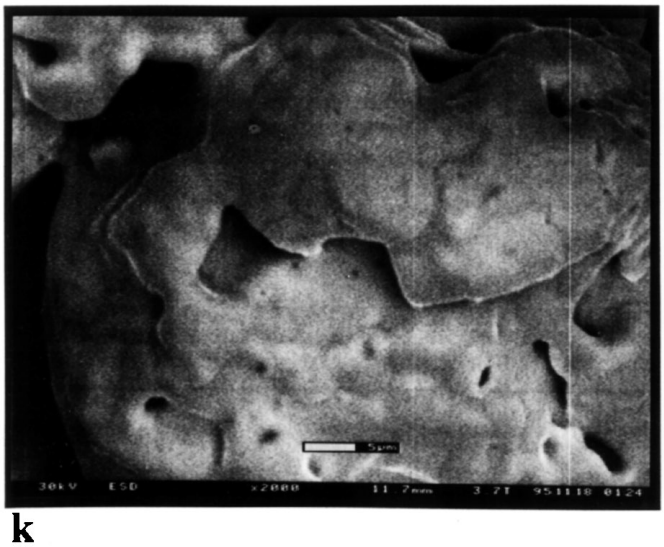

k

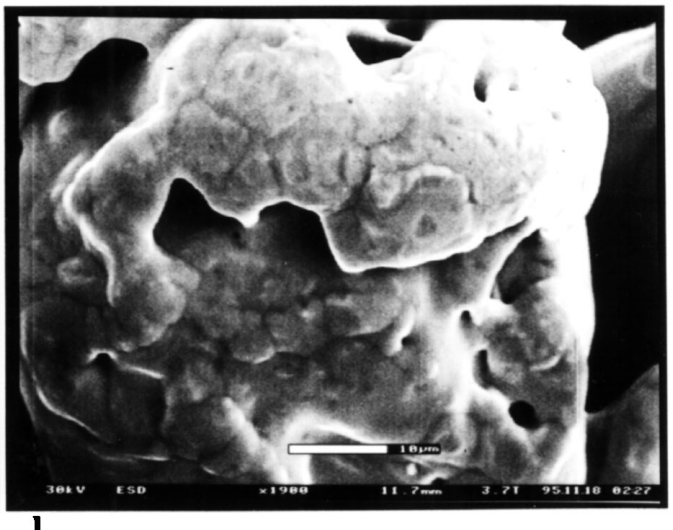

l

FIG. 4—*Continued*

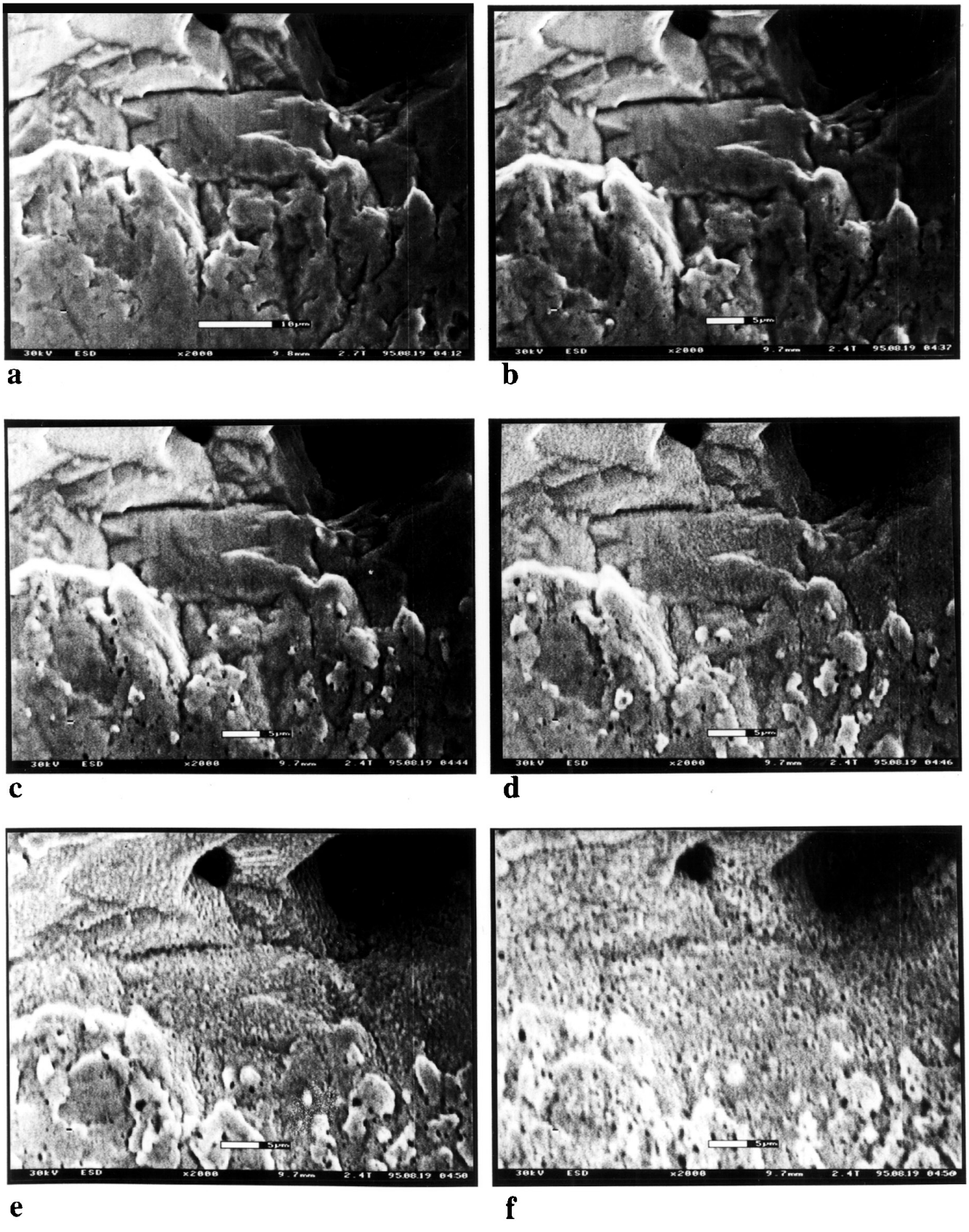

FIG. 5. Real time ESEM images of polycrystalline silver catalyst in methanol/air mixture at (a) 298, (b) 713, (c) 813, (d) 843, (e) 873, (f) 908, (g) 928, (h) 943, and (i) 965 K. The catalyst was then held at this temperature in the presence of the reaction mixture for a further time of (j) 13, (k) 27, and (l) 41 min.

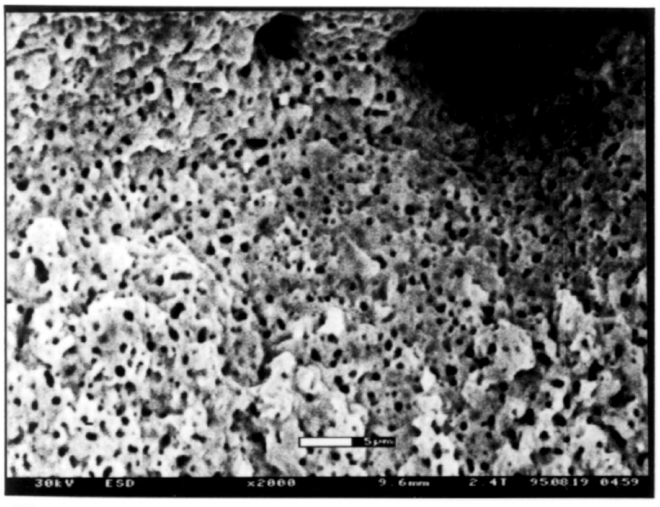

g

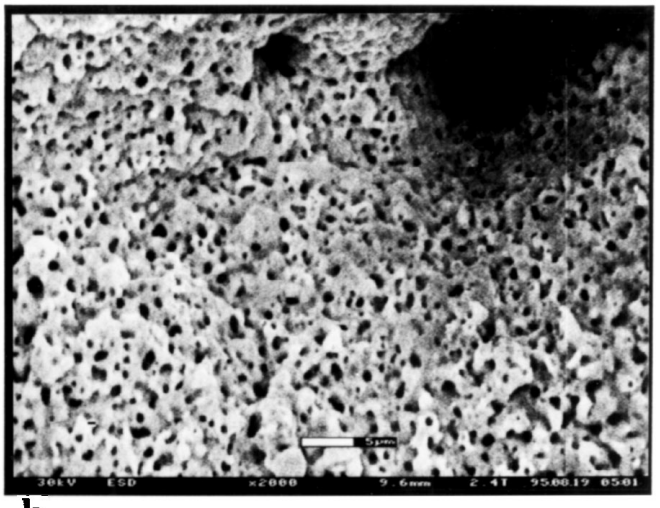

h

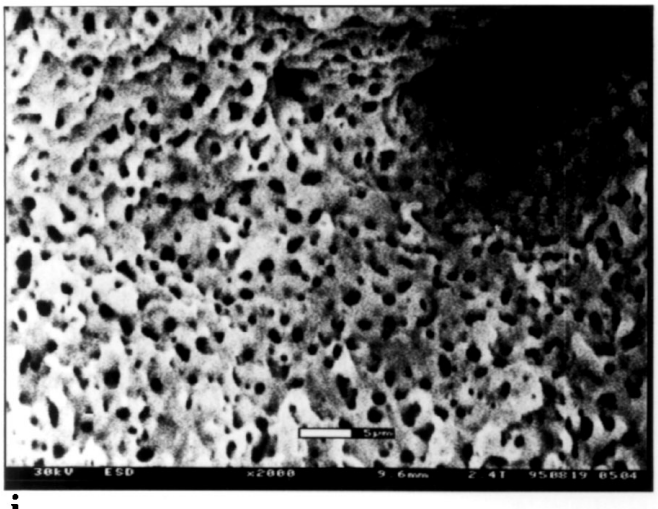

i

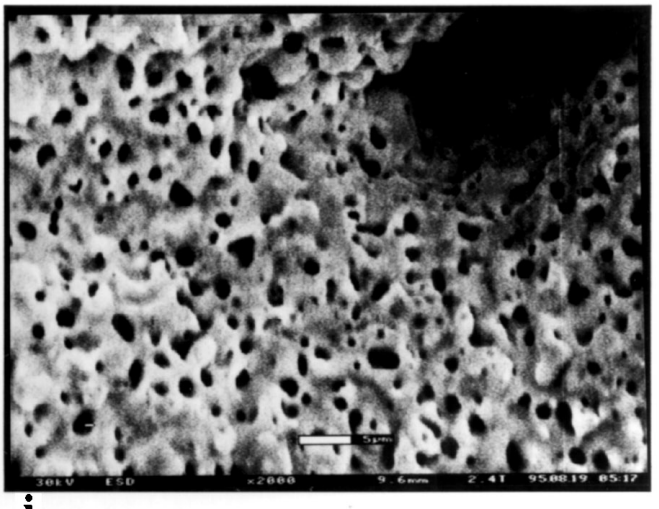

j

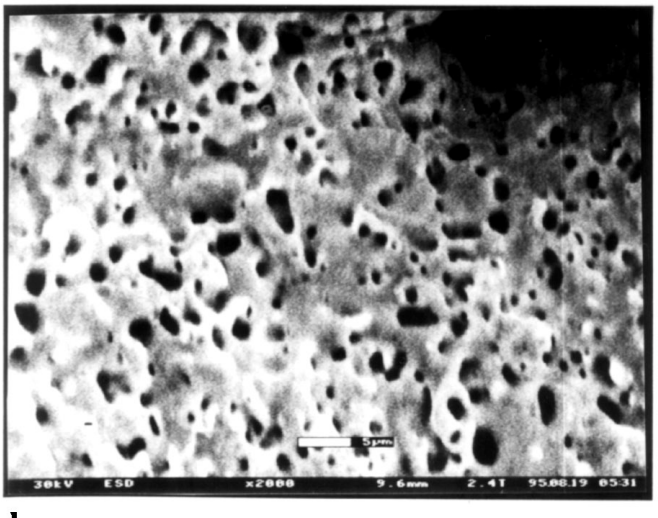

k

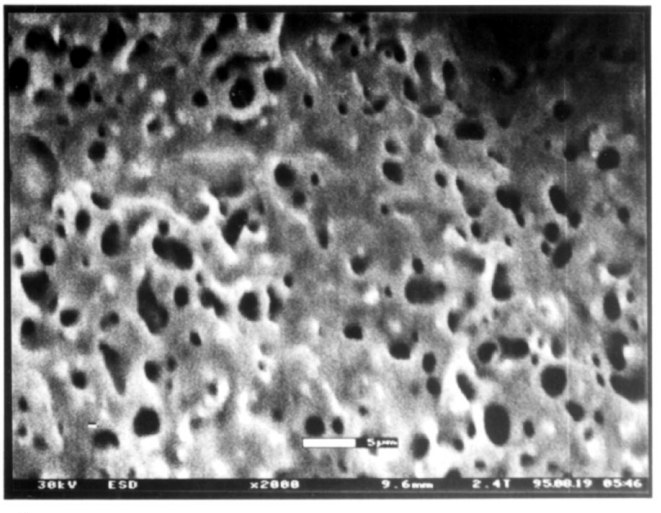

l

FIG. 5—*Continued*

in the vicinity of defects on the silver surface. Lefferts *et al.* (29) recorded that the desorption of water from a silver catalyst occured at ca. 400–450°C (673–723 K), if subsurface hydroxyl species were present. Moreover, it was proposed that these hydroxyl species were located in the vicinity of surface defects (14, 29). Millar *et al.* (22) noted the detection of an intense Raman band at ca. 451 cm^{-1} during the methanol oxidation reaction on polycrystalline silver which disappeared at a temperature of ca. 673 K. Electron microscopy images have shown that surface explosion had occurred, as evidenced by the debris surrounding each "pinhole" (16). Bao *et al.* (15) proposed that interaction between subsurface hydrogen and oxygen species produced water which exerted considerable hydrostatic pressure. Consequently, it is concluded that the pinholes detected in Figs. 5b and 5c, were either caused by the recombination of subsurface hydroxyl groups or the reduction of subsurface hydroxyl species by adsorbed hydrogen, situated at defect sites, subsequently forming water vapor which erupted through the silver surface.

Further heating (Fig. 5c) resulted in an increase in the size of the "pinholes" and also the formation of platelets on the silver surface became visible. At the edge of each platelet feature were "pinholes" which suggested an intimate relationship between the appearance of platelets and "pinholes." Widespread changes in the appearance of the silver surface were initiated at 843 K (Fig. 5d). The entire structure became covered with small "nodules," an effect which has not previously been recorded. As the reaction progressed, the "nodules" become more substantial in size and further hole evolution started (Fig. 5e). Violent eruptions to produce micrometer sized holes over the entire catalyst surface were imaged at 908 K (Fig. 5f) and it was noted that these holes originated at the sites where "nodules" had been created. Extension of the reaction time resulted in the dimension of the holes ever increasing, ultimately to values in the range 1–5 μm (Figs. 5g–5l). However, this was not the only effect observed as it could also be seen that the surface was now extremely mobile (note the disappearance of the large hole in the upper middle section of Fig. 5 with time). During imaging it was possible to monitor the appearance and subsequent destruction of a "pinhole." Furthermore, a series of small holes could be seen to amalgamate to form larger defect structures. An intriguing observation was the development of relatively smooth areas on the silver catalyst as the reaction progressed (Figs. 5k and 5l). Finally, it is emphasized that of the complex behavior recorded in Fig. 5 only the low temperature effects were noted when methanol was introduced to the system, therefore the vast structural reconstruction observed at high temperature must have been due to another form of catalytic etching.

Images of the silver catalyst before and after the methanol oxidation process, from a variety of different grain types in the sample were carefully examined. It was evident that in this case the entire silver surface reacted with the O_2/CH_3OH mixture, suggesting that this catalyst was very active towards methanol oxidation. Data from an industrial plant concerning the activity of the catalyst used in this study supported this conclusion as significant formaldehyde formation was shown to be rapidly achieved (for proprietary reasons the precise information cannot be released). Furthermore, upon opening the ESEM chamber after the experiment the pungent aroma of formaldehyde was apparent.

Raman microscopy was performed on the silver catalyst following the methanol oxidation reaction in order to determine which chemisorbed species were present (Fig. 6). Figure 6a contains bands at ca. 230, 462, 487, 544, 610, and 678 cm^{-1}, whereas a second location (Fig. 6b) exhibited peaks at 260, 429 cm^{-1} and a broad envelope between ca. 500 and 700 cm^{-1}, in addition to features at ca. 820 and 897 cm^{-1}. The strong band at 230 cm^{-1} (Fig. 6) indicated the presence of adsorbed molecular oxygen which probably arose as a consequence of readsorption of oxygen during cooling of the catalyst to room temperature. Similarly, the detection of a band at 897 cm^{-1} (Fig. 6b) ascribed to molecular oxygen bound to reconstructed silver sites may have been formed at lower temperature also. The known stability of these species (30) dictates that their concentration should be extremely small under the reaction conditions employed here. The observation of the peak at 678 cm^{-1} probably indicated the presence of carbonate species on the silver surface (22) but again it must be concluded that their formation occurred primarily as a consequence of adsorption of adventitious CO_2 at ambient temperature. The sharp peak at 462 cm^{-1} (Fig. 6a) is characteristic for subsurface hydroxyl located at defect sites (22). In accordance with the enhanced defecting of the silver surface following reaction, it is considerably more intense than the weak maxima observed for subsurface hydroxyl on the fresh catalyst (Figs. 1a and 1b). The band at ca. 544 cm^{-1} is also indicative of subsurface hydroxyl species beneath the smoother areas of the catalyst surface.

The existence of dissolved oxygen in the bulk silver structure has been proposed by several authors (14, 22) and structures comparable to silver(I) oxide are identified by a band at ca. 485 cm^{-1} (22) (note that Ag_2O and AgO are not stable at the high temperature conditions used for methanol oxidation). The band determined at ca. 487 cm^{-1} is in excellent agreement with this value and therefore is indicative of the formation of more extensively dissolved oxygen atoms during the methanol oxidation reaction. Lefferts *et al.* (14, 29) postulated that defects in the silver structure facilitated the diffusion of oxygen into the bulk lattice. This theory is in accordance with our data which show a correlation between the appearance of the band at 487 cm^{-1} and defect production.

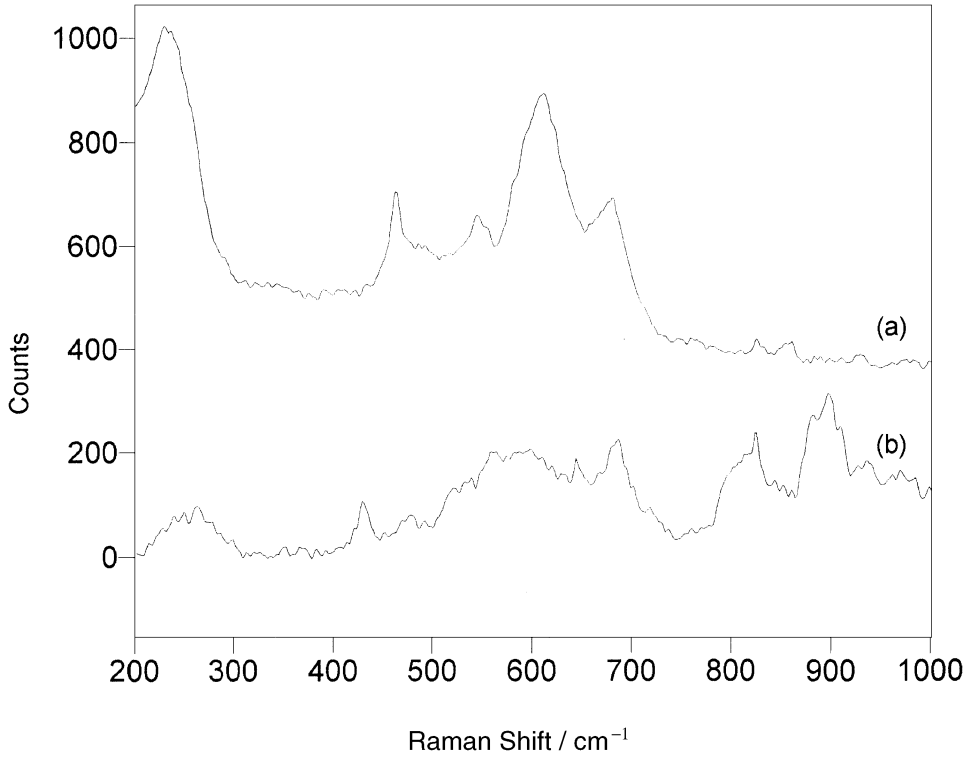

FIG. 6. Raman spectra of two locations on the surface of polycrystalline silver after exposure of methanol/air at 965 K in the ESEM chamber.

DISCUSSION

Raman spectroscopy has revealed that when silver catalysts are synthesized by electrochemical methods, a variety of oxygen species become incorporated in the sample (Fig. 1). The identification of subsurface hydroxyl and oxygen species plus strongly bound atomic oxygen suggests that a fraction of the silver surface is already in a reconstructed state similar to that reported by Bao *et al.* (7). In harmony with this conclusion was the observation of a band at 965 cm^{-1} typical for the ν(O–O) mode of adsorbed molecular oxygen on oxidised silver sites (22). The analysis of Wang *et al.* (31) indicates that the charge on the molecular oxygen was ca. 1.25 electrons, i.e. it is essentially an "O_2^-" species. Previously, Millar *et al.* (22) proposed that molecular oxygen was stabilized by adsorption at Ag^+ sites to produce an "$Ag^{2+}\,O_2^-$" complex. Furthermore, Wu *et al.* (32) advanced the idea that the stabilization of molecular oxygen is intimately related to the presence of surface defects in the silver structure. In relation to the latter theory, it is noted that even in spectra where the 965 cm^{-1} band is absent, there is still considerable Raman scattering in the range 200–240 cm^{-1} (Figs. 1c and 1d). This observation suggests that a substantial concentration of weakly bound molecular oxygen species may also exist. Sexton and Madix (20) assigned an EELS feature at 240 cm^{-1} to the ν(Ag–O_2) vibration of weakly adsorbed molecular oxygen on silver, hence our deduction appears to be supported.

Environmental scanning electron microscopy (ESEM) has been shown to be an exceptionally powerful means for imaging structural changes induced by catalytic etching in a silver catalyst (cf. Figs. 4 and 5). The first change recorded in the silver surface during methanol oxidation was the appearance of "pinholes" at 713 K (Fig. 6b). Lefferts *et al.* (14) reported the desorption of water between 673 and 723 K if subsurface hydroxyl species were present. Miller *et al.* (22) also noted the growth of a Raman band at 451 cm^{-1} (assigned to the ν(OH) vibration of a subsurface hydroxyl species) during methanol oxidation on silver at 473 K, which subsequently disappeared at 673 K. This latter observation was in excellent agreement with the formation of "pinholes" imaged by ESEM and resultant water production analysed by a TCD (14). Further investigation using ESEM has shown that "pinholes" were indeed formed on the edges of surface defects in the silver catalyst employed in the previous study (33). Lefferts *et al.* (14, 29) proposed that the subsurface hydroxyls detected in their study were created at defect sites. Wu *et al.* (32) have also emphasised the importance of surface defects in allowing formation of subsurface oxygen species in silver. Additionally, Meima *et al.* (34) noted that substantial oxygen penetration can occur at grain boundaries and surface defects. Consequently, we propose that the following

reactions occurred at defect sites

$$CH_3OH(ads) + O(def) \Rightarrow CH_3O(ads) + OH(def)$$
$$OH(def) + OH(def) \Rightarrow H_2O(g) + O(def).$$

In agreement with Bao *et al.* (15) the resulting hydrostatic pressure is proposed to create stress which is ultimately released via a surface explosion. Recently, evidence of debris formation in the area of pinholes was obtained which supported the hypothesis that eruptions in the silver catalyst had occurred (16).

As the methanol oxidation reaction proceeded (Fig. 5c) the size of the pinholes gradually increased. This effect may indicate that once pinholes were produced they then acted as defect sites which further allowed oxygen species to enter subsurface locations. Again, reaction with methanol to form subsurface OH species happened and finally recombinative desorption of subsurface OH caused more extensive defect formation. This proposal is in accord with the mechanism suggested by Bao *et al.* (15) for the life cycle of a silver catalyst under simultaneously oxidising and reducing atmospheres.

Substantial platelet formation was also clearly observed (Figs. 5c and 5d), an effect not previously reported. Clearly, a relationship existed between "pinhole" creation and the appearance of the platelets, since pinholes were always detected on the edge of these latter structures. It is postulated that significant penetration of oxygen and subsurface hydroxyl species into the bulk silver structure occurred at defect sites. Subsequent water production produced a pressure which was then sufficient to dislodge large areas of silver during the eruption process, thus forming platelets. As the catalyst temperature increased to 843 K, small "nodules" developed over the entire silver surface (Fig. 5d). These "nodules" became more prominent as the temperature was raised to 873 K (Fig. 5e), and eventually pinholes evolved in the vicinity of each "nodule." This behaviour indicated that substantial concentrations of subsurface hydroxyl species were "stored" in each "nodule." Lefferts *et al.* (14) provided evidence for two distinct hydroxyl species in polycrystalline silver by using TPR methods. Hydroxyl species present at defect sites were reduced at ca. 673 K whereas subsurface oxygen was reduced at 823 K. It is interesting that the "nodules" first appear at temperatures in excess of ca. 773 K, since Bao *et al.* (28) have shown that significant oxygen reconstruction of a silver (111) single crystal is initiated at 800 K. Once subsurface oxygen is formed it can then subsequently react with methanol to again produce subsurface hydroxyl. As this effect is now widespread across the silver surface, it is reasonable to assume that considerable surface stress is produced.

There exist two means by which surface stress could be reduced in this instance: (1) by reconstruction of the silver to a form which minimises the surface free energy, e.g. in the simplest case a "hill and valley" structure, or (2) by surface explosions to form pinholes. In this case, these two processes appeared to happen sequentially.

It is of considerable interest to compare and contrast the behaviour of the silver catalyst in the presence of either methanol or methanol/oxygen with the recent activity data provided by Schubert *et al.* (35). The efficiency of conversion to formaldehyde of a commercial polycrystalline silver catalyst used for methanol oxidation was reported. At the optimum methanol/oxygen ration (1.25) it was noted that the formaldehyde conversion exhibited a sharp increase (from ca. 4 to 42%) in the temperature range 720–765 K. The conversion efficiency then remained comparatively stable until the catalyst attained a temperature of ca. 825 K, whereupon the conversion to formaldehyde rapidly increased from ca. 44 to 70% (by 865 K). In contrast, in methanol rich conditions (CH_3OH/O_2 ratio 1.8), although the first increase in conversion efficiency at ca. 720–765 K was recorded, the second increase at ca. 825 K was not. Moreover, the conversion efficiency actually decreased markedly at 825 K, eventually reaching a value of only 16% at 950 K. Consequently, it was relevant to compare the "pinhole" concentration observed by ESEM for the silver catalyst with the activity data reported by Schubert *et al.* (35). Figure 7 reveals a strong correlation between the conversion efficiency to formaldehyde for a silver catalyst (from the data of Schubert *et al.* (35)) and the extent of hole formation on the catalyst surface. One aspect to note is that although there was a tenfold increase in "pinhole" concentration once the temperature was raised to ca. 655 K during methanol oxidation conditions (Fig. 9) the activity as reported by Schubert *et al.* (35) did not proportionately

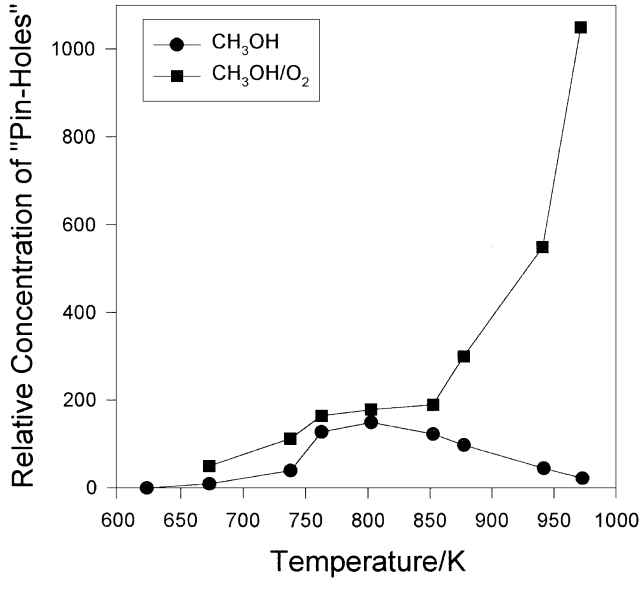

FIG. 7. Comparison of the extent of hole production observed during the ESEM study of silver in the presence of methanol and methanol/air.

increase. This behaviour may indicate the participation of surface atomic oxygen in the reaction at low temperatures since the following proposed mechanism would not result in any "pinhole" formation and therefore would go undetected by ESEM:

$$CH_3OH(ads) + O(ads) \Rightarrow OH(ads) + CH_3O(ads)$$
$$CH_3O(ads) \Rightarrow CH_2O(ads) + H(ads).$$

Schubert *et al.* (35) reported that the reaction with surface oxygen was of limited selectivity, a point also emphasised by Lefferts *et al.* (29) who indicated that weakly bound oxygen was the cause of methanol combustion. The mechanism for this process can be deduced from the data of Wachs and Madix (9) and Lefferts *et al.* (5, 29).

$$CH_2O(ads) + O(ads) \Rightarrow CH_2OO(ads)$$
$$CH_2OO(ads) \Rightarrow HCOO(ads) + H(ads)$$
$$2HCOO(ads) \Rightarrow 2CO_2(g) + H_2(g)$$

The relationship between "pinhole" production in the vicinity of defects and the enhanced formaldehyde selectivity in the low temperature range strongly supports the conclusion that methanol interaction with subsurface oxygen (or subsurface hydroxyl groups) at defect sites only results in formaldehyde formation, with no overoxidation products. This effect can be explained in terms of steric considerations. Previous studies involving the infrared probing of a polycrystalline silver catalyst with formic acid revealed the presence of three distinct chemisorbed formate species (8). One of these formate species was located on reconstructed silver crystal planes whereas the remaining two species were adsorbed on low-index silver crystal faces. Significantly, upon desorption of these formate species it was discovered that coadsorbed oxygen destabilized only those species bonded to the low-index silver planes (the degree of destabilization depending upon the number of neighbouring oxygen atoms). Consequently, it was deduced that although formic acid could dissociatively adsorb on an oxygen reconstructed silver surface, once the formate was formed the C–H bond was now sterically too far from the subsurface oxygen species to be "attacked" during desorption (8). Therefore, we can infer that a similar effect occurs during the methanol oxidation reaction.

The second plateau in "pinhole" production which correlated to a concomitant increase in methanol conversion to formaldehyde (Fig. 7) has been aligned with the incorporation of oxygen into the subsurface region of silver (28). This theory is in accordance with the ESEM data which showed the formation of "nodules" over the entire silver surface at temperatures in excess of ca. 823 K (Fig. 5) which were indicative of the presence of oxygen species in the near-surface region of silver. Once subsurface oxygen is present

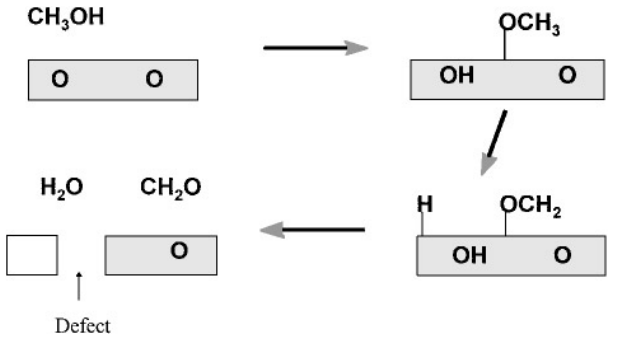

FIG. 8. Diagrammatic representation of the surface interaction of methanol with subsurface oxygen species located in the uppermost layer of silver. The subsurface hydroxyl species produced subsequently recombine with either adsorbed hydrogen or hydroxyl species to make water which then erupts through the surface to make pinhole defects.

it can react with methanol as

$$CH_3OH(ads) + O(sub) \Rightarrow CH_3O(ads) + OH(sub)$$
$$CH_3O(ads) \Rightarrow CH_2O(ads) + H(ads)$$
$$OH(sub) + OH(sub) \Rightarrow H_2O(sub) + O(sub)$$
$$H(ads) + OH(sub) \Rightarrow H_2O(sub)$$
$$H_2O(sub) \Rightarrow H_2O(g) + \text{"pinhole"}$$
$$H(ads) + H(ads) \Rightarrow H_2(g),$$

and we have also presented these reactions diagrammatically in Fig. 8. The high selectivity to formaldehyde reported by Schubert *et al.* (35) (which was confirmed by data from an actual industrial plant for the catalyst used in this study) is again easily rationalised in terms of the aforementioned argument regarding steric accessibility of oxygen. As demonstrated by Ertl and co-workers (7), subsurface oxygen species are nucleophilic in character, as are the surface atomic oxygen species (albeit to a lesser degree). Therefore, the most plausible reason for subsurface oxygen species to be highly selective to formaldehyde has to be that they are sterically hindered from further attacking the formaldehyde product.

CONCLUSIONS

1. Polycrystalline silver catalysts produced by electrochemical methods contain significant concentrations of a variety of oxygen species. Raman microscopy revealed that they are not homogeneously distributed over the entire silver surface. Instead, it appears that they are located at specific locations, such as grain boundaries and other related defect structures.

2. The interaction of oxygen and/or water with polycrystalline silver results in surface reconstruction due primarily to incorporation of oxygen species into subsurface sites.

3. Extensive etching of silver is induced only by the presence of both methanol and oxygen in the reaction mixture. Two distinct active sites were discerned using ESEM, one at defect sites and the second on planes reconstructed by subsurface oxygen. It was only during methanol oxidation conditions that "pinhole" formation, caused by recombination of subsurface hydroxyls to make water, was noted.

4. The surface of silver catalyst was observed to be extremely mobile during typical industrial reaction conditions.

5. A correlation between formaldehyde formation and "pinhole" production was developed. A hypothesis regarding the steric inaccessibility of subsurface oxygen species restricting further attack of product formaldehyde was provided to explain why an oxygen reconstructed silver surface should be selective.

REFERENCES

1. Lafyatis, D. S., Creten, G., and Froment, G. F., *Appl. Catal.* **120**, 85 (1994).
2. Sperber, H., *Chemie-Ing-Techn.* **41**, 962 (1969).
3. Sajkowski, D. J., and Boudart, M., *Catal. Rev. Sci. Eng.* **29**, 325 (1987).
4. van Santen, R. A., and Kuipers, P. C. E., *Adv. Catal.* **35**, 265 (1987).
5. Lefferts, L., van Ommen, J. G., and Ross, J. R. H., *Appl. Catal.* **23**, 385 (1986).
6. Deng, J., Xu, X., Wang, J., Liao, Y., and Hong, B., *Catal. Lett.* **32**, 159 (1995).
7. Bao, X., Muhler, M., Pettinger, B., Schlögl, R., and Ertl, G., *Catal. Lett.* **22**, 215 (1993).
8. Millar, G. J., Metson, J. B., Bowmaker, G. A., and Cooney, R. P., *J. Catal.* **147**, 404 (1994).
9. Wachs, I. E., and Madix, R. J., *Surf. Sci.* **76**, 531 (1978).
10. Rovida, G., Pratesi, F., Maglietta, M., and Ferroni, E., *Surf. Sci.* **43**, 230 (1974).
11. Plischke, J. K., and Vannice, M. A., *Appl. Catal.* **42**, 255 (1988).
12. Rhead, G. E., and Mykura, H., *Act. Metall.* **10**, 843 (1962).
13. Meima, G. R., Vis, R. J., van Leur, M. G. J., van Dillen, A. J., Geus, J. W., and van Buren, F. R., *J. Chem. Soc. Faraday Trans. 1* **85**, 279 (1989).
14. Lefferts, L., van Ommen, J. G., and Ross, J. R. H., *Appl. Catal.* **34**, 329 (1987).
15. Bao, X., Lehmpfuhl, G., Weinberg, G., Schlögl, R., and Ertl, G., *J. Chem. Soc. Faraday Trans.* **88**, 865 (1992).
16. Millar, G. J., Nelson, M. L., and Uwins, P. J. R., *J. Chem. Soc. Faraday Trans.*, in press.
17. Uwins, P. J. R., *Mater. Forum* **18**, 51 (1994).
18. Kondarides, D. I., Papatheodorou, G. N., Vayenas, C. G., and Verykios, X. E., *Ber. Bunsenges Phys. Chem.* **97**, 709 (1993).
19. Benndorf, C., Franck, M., and Thieme, F., *Surf. Sci.* **128**, 417 (1983).
20. Sexton, B. A., and Madix, R. J., *Chem. Phys. Lett.* **76**, 294 (1980).
21. Maynard, K. J., and Moskovits, M., *J. Chem. Phys.* **90**, 6668 (1989).
22. Millar, G. J., Metson, J. B., Bowmaker, G. A., and Cooney, R. P., *J. Chem. Soc. Faraday Trans.* **91**, 4149 (1995).
23. Bao, X., Pettinger, B., Ertl, G., and Schlögl, R., *Ber. Bunsenges. Phys. Chem.* **97**, 322 (1993).
24. Pettinger, B., Bao, X., Wilcock, I. C., Muhler, M., and Ertl, G., *Phys. Rev. Lett.* **72**, 1561 (1994).
25. Bao, X., Muhler, M., Pettinger, B., Uchida, Y., Lehmpfuhl, G., Schlögl, R., and Ertl, G., *Catal. Lett.* **32**, 171 (1995).
26. Millar, G. J., Nelson, M. L., and Uwins, P. J. R., *Catal. Lett.* **43**, 97 (1997).
27. Carter, E. A., and Goddard, W. A., *Surf. Sci.* **209**, 243 (1989).
28. Bao, X., Barth, J. V., Lehmpfuhl, G., Schuster, R., Uchida, Y., Schlögl, R., and Ertl, G., *Surf. Sci.* **284**, 14 (1993).
29. Lefferts, L., van Ommen, J. G., and Ross, J. R. H., *Appl. Catal.* **31**, 291 (1987).
30. Barteau, M. A., and Madix, R. J., *Surf. Sci.* **97**, 101 (1980).
31. Wang, X. D., Tysoe, W. T., Greenler, R. G., and Truszkowska, K., *Surf. Sci.* **258**, 335 (1991).
32. Wu, K., Wang, D., Wei, X., Cao, Y., and Guo, X., *J. Catal.* **140**, 370 (1993).
33. Millar, G. J., Nelson, M. L., and Uwins, P. J. R., unpublished results.
34. Meima, G. R., Vis, R. J., van Leur, M. G. J., van Dillen, A. J., Geus, J. W., and van Buren, F. R., *J. Chem. Soc. Faraday Trans.* **85**, 279 (1989).
35. Schubert, H., Tegtmeyer, U., Herein, D., Bao, X., Muhler, M., and Schlögl, R., *Catal. Lett.* **33**, 305 (1995).